Chemical Engineering Journal 415 (2021) 128988

Contents lists available at ScienceDirect

Chemical Engineering Journal

journal homepage: www.elsevier.com/locate/cej

Asymmetric bilayer CNTs-elastomer/hydrogel composite as soft actuators with sensing performance

Huijing Li [a,b], Yun Liang [a,b], Guorong Gao [a,b], Shuxin Wei [a,b], Yukun Jian [a,b], Xiaoxia Le [a,b], Wei Lu [a,b], Qingquan Liu [c], Jiawei Zhang [a,b,*], Tao Chen [a,b,*]

[a] Key Laboratory of Marine Materials and Related Technologies, Zhejiang Key Laboratory of Marine Materials and Protective Technologies, Ningbo Institute of Material Technology and Engineering, Chinese Academy of Sciences, Ningbo 315201, China
[b] School of Chemical Science, University of Chinese Academy of Sciences, 19A Yuquan Road, Beijing 100049, China
[c] School of Materials Science and Technology, Hunan Provincial Key Laboratory of Advanced Materials for New Energy Storage and Conversion, Hunan University of Science and Technology, Xiangtan 411201, China

ARTICLE INFO

Keywords:
Soft actuator
Integrated sensor
CNTs
PNIPAm hydrogel

ABSTRACT

Living creatures have the nature of actuating and sensing under external stimuli to better adapt to the environment. For instance, the combination of muscles actuation and skin sensing ensures our intelligent interaction with external environments. In terms of the soft robot, implanting sensation and actuation in one system can assist us to control it better and more efficiently. However, in the development of biomimetic materials, the simultaneous realization of actuating and sensing performance in bionic soft robots is still a great challenge. Here, we propose a novel asymmetric bilayer CNTs-elastomer/PNIPAm hydrogel composite with integrated actuating and sensing performances. Due to the excellent photothermal effect of CNTs and thermo-responsiveness of PNIPAm, under the NIR irradiation, the PNIPAm hydrogel layer would shrink and the bilayer composite would thus perform a bending deformation. At the same time, based on a piezoresistive sensing mechanism of the CNTs-elastomer, the actuating procedure can be recorded. This work may open up a new insight in the designing and fabricating intelligent biomimetic hydrogel soft robots with integrated self-sensing capacity.

1. Introduction

As one of the most promising biomimetic intelligent materials, polymeric hydrogel actuators could generate reversible shape transformation upon the trigger of various external stimuli, such as temperature [1,2], pH [3–6], light [7–9], chemicals [10], electric field [11,12] etc. Therefore, they have attracted considerable interest and shown potential applications as artificial muscles [11], on-off switches [13,14], soft robots [8,15,16] and so on. After decades of development, the hydrogel actuators now could produce complex shape deformations [17,18]. Moreover, fluorescence color-changing [19,20], shape memory performances [21,5] have been incorporated to fabricated multifunctional hydrogel actuators. However, the shape transformation process of hydrogel actuators is often recorded by camera, which is inefficient and limited by lighting situations. On the other hand, living creatures have sensing ability during the movement, which is more conducive for their adaptation to the environment. Therefore, hydrogel actuators with integrated sensing performance can produce real-time feedback signals during the actuating procedure, which could expand its potential applications.

To produce shape deformation, a commonly used method is fabricating bilayer structures, with one layer that could swell or shrink upon external stimuli as the active layer, and another layer that does not change with the external environment as the passive layer. Besides hydrogel [22–24], paper [20], elastomers [6] which are stable in various evironments and mechanically robust could also be applied as passive layer to construct a hydrogel-based actuator with shape deformation performance. For instance, Zhou and co-workers have attached hydrogel layer on PDMS sheet to achieve fast actuating performance [25]. Moreover, compared with other stimuli, light is remotely-controllable. To realize light controllable deformation, there are a number of materials with photothermal conversion have been added into hydrogel actuators, such as GO [26], gold [27,28], Fe_3O_4 nanoparticles [29], polypyrrole [30] and so on. Here, CNTs was chosen as photothermal

* Corresponding authors.
E-mail addresses: zhangjiawei@nimte.ac.cn (J. Zhang), tao.chen@nimte.ac.cn (T. Chen).

https://doi.org/10.1016/j.cej.2021.128988
Received 20 October 2020; Received in revised form 10 January 2021; Accepted 10 February 2021
Available online 16 February 2021

conversion material which is conductive as well, so that the actuation can be sensed at the same time. It could imagine if a sensing component is incorporated into the hydrogel-based actuator, the shape transformation process could be detected in real time. Furthermore, according to the feedback signal, the actuating process can be controlled more efficiently.

Herein, we report a novel hydrogel composite actuator with integrated shape deformation and sensing behaviors. As shown in Fig. 1a, the asymmetric bilayer CNTs-elastomer/hydrogel composite realizes the combination of sensing and actuating function which is similar to the collaboration between skin and muscles. The CNTs/Ecoflex layer is applied as the sensing layer, while the thermo-responsive PNIPAm hydrogel is applied as the actuation active layer to generate contraction upon the trigger of heat, with the ability to move similar to muscles. Under the irradiation of NIR, light is converted to heat because of the near-infrared (NIR) photothermal effect of CNTs, and the PNIPAm layer shrinks because of the loss of water, the bilayer hydrogel composite bends toward the PNIPAm layer as a result. Moreover, the CNTs/Ecoflex film is also conductive, resulting that asymmetric bilayer CNTs-elastomer/hydrogel composite possesses sensing performances which acts as "skin" in this system. Therefore, the CNTs/Ecolflex layer could generate electrical signals due to the stretch caused by bending, and thus the actuating process could be monitored in real time.

2. Experimental section

2.1. Materials

The raw carbon nanotubes (CNTs) (diameter, about 8–15 nm; length, about 50 μm; –COOH %, about 1.23 wt%) with purity of over 98% were purchased from Chengdu Organic Chemistry Co., Ltd., and were rinsed thoroughly with anhydrous ethanol and dried in a stream of nitrogen before use. Silicon rubber (Ecoflex 00-30) was purchased from Smooth-on, USA. Other analytical reagent grade solvents and reagents were obtained from Sinopharm Chemical Reagent Co. Ltd., Shanghai and used as received. The Milli-Q-grade water was used to prepare CNTs-Ecoflex Janus hybrid film at the air/water interface. *N*-isopropyl acrylamide (NIPAm), 2-hydroxy-4′-(2-hydroxyethoxy)-2-methylpropiophenone (I2959), *N*,*N*′-methylenebis (acrylamide) (Bis) and benzophenone were obtained from Aladdin reagent Co. Ltd, Shanghai.

2.2. Preparation of CNTs film

According to previous Langmuir-Blodgett assembled methods, the CNTs films at the air/water interface were prepared. Typically, 400 mg the pre-prepared CNTs were dispersed with 200 mL anhydrous ethanol, and the mixture was sonicated for 2 h to form a stable dispersion. Afterwards, the resultant uniform CNTs dispersion was spread onto the water surface by a spray-coating method, and a uniform pre-assembled film formed at the air/water interface. Eventually, after stabilized for about 30 min, the capillary substances like tissue or microporous sponges were selected to put on one side of the interface to realize quickly siphon water from the system, meanwhile, the area of the pre-assembled CNTs film decreased. Notably, the homogeneous preassembled CNTs layers were closely packed toward the opposite direction of the siphon situation. When the compression of the film stopped and sponges could not compress the film further, the resulting film was finally formed, indicating a closely packed structure.

2.3. Preparation of ultrathin CNTs/Ecoflex Janus film

The prepolymer and cross-linker of Ecoflex were mixed in a 1:1 (w/w) ratio, then they were diluted by *N*-heptane with a weight ratio of 4%. The obtained mixture solution was sprayed onto the surface of the as-

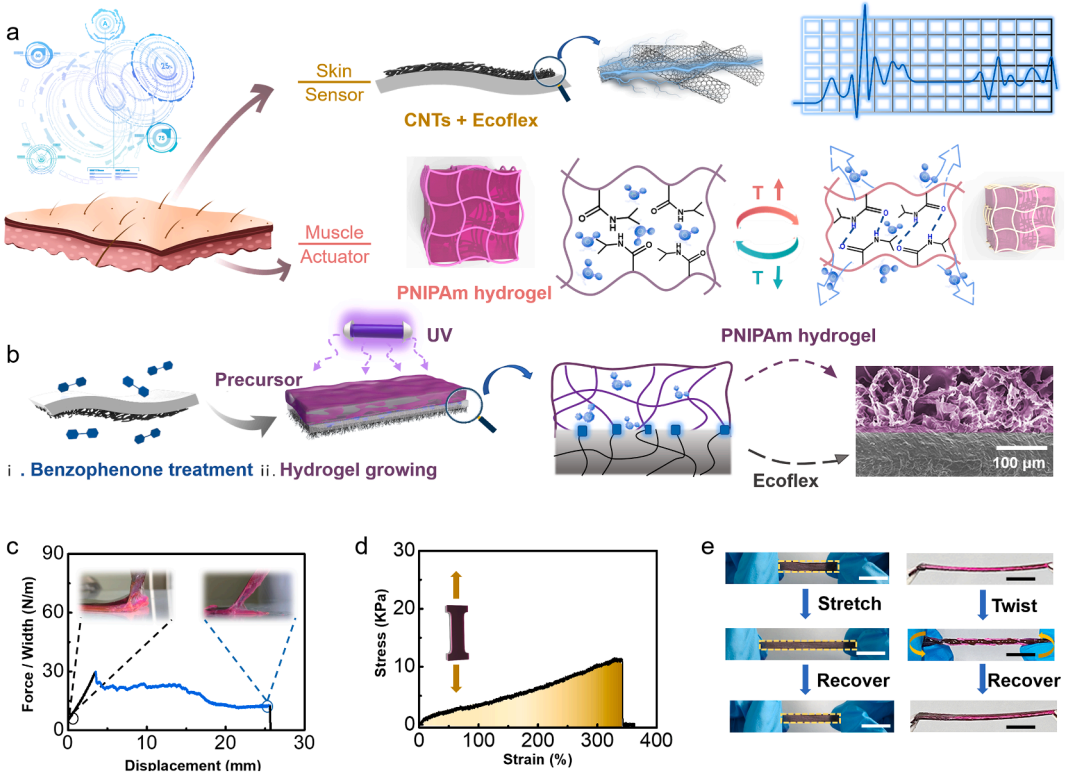

Fig. 1. (a) The illustration of skin and muscle inspired CNTs-Ecoflex/PNIPAm hydrogel composite that can actuate and self-sensing. (b) Schematic of the fabrication and the structure of CNTs-Ecoflex /PNIPAm hydrogel composite. (c) The curve of the peeling force per width of CNTs-Ecoflex /PNIPAm hydrogel composite sheet versus displacement for interface bonding and photos of peeling process. (d) The tensile stress-strain curve of CNTs-Ecoflex/PNIPAm hydrogel composite film. (e) Photos of CNTs-Ecoflex /PNIPAm hydrogel composite before and after stretching and 20 cycles of continuous twisting tests.

prepared CNTs film directly to achieve a uniform layer, followed by a typical Ecoflex curing process at room temperature for 6 h and the CNTs-Ecoflex ultrathin Janus film was obtained at air/water interface. At the end of stage, the CNTs-Ecoflex ultrathin Janus film was transferred on PET film.

2.4. Preparation of the CNTs-Ecoflex/hydrogel composite

First of all, the CNTs-Ecoflex ultrathin Janus film was treated by dipping into a 2 wt% ethanol solution of benzophenone. NIPAm monomers (1 g), Bis (10 mg), and I2959 (10 mg) were dissolved in 8 mL of deionized water and stirred to obtain a homogenous precursor. Afterwards, the hydrogel precursor was poured onto the above CNTs-Ecoflex film which was pressed and fixed by a layer of silica plate, at the same time, they were sealed between two glass plates (2 mm). Subsequently, followed by ultraviolet irradiation (365 nm) for 10 min, the PNIPAm hydrogel was covalently crosslinked and bonded onto the Ecoflex surface (as show in Fig. S1).

2.5. Characterization

Scanning electron microscopy (SEM) was performed to observe the micromorphology of CNTs-Ecoflex/PNIPAm film with a Hitachi S-4800 cold field emission SEM at an accelerating voltage of 10 kV. When characterization of the sensing performance of the CNTs-Ecoflex/PNIPAm hydrogel composite, a Zwick Z1.0 universal testing machine was used to stretch rectangular CNTs-Ecoflex/PNIPAm hydrogel composite specimens (15 mm × 3 mm) with one end fixed and another one linearly elongated at a constant speed. Resistance measurements were carried out by connecting the two ends of the CNTs-Ecoflex/PNIPAm film to a Electrochemical Workstation (CH Instruments, CHI660E. Chenhua Co., Shanghai, China), with conductive copper wires to record the real-time resistance (I) flowing through the film under a constant voltage (U_0) of 1 V, while the real-time resistance (R) was calculated by the equation $R = U_0/I$. The arm model was made by PET tubes.

3. Results

3.1. Strong adhesion between hydrogel layer and CNTs-Ecoflex hybrid

The preparation of the bilayer CNTs-Ecoflex/PNIPAm hydrogel composite is illustrated in Figs. 1b and S1. First of all, CNTs thin film was prepared on an air/water interface through capillary force driving compression according to previous methods [31], then the solution of Ecoflex was sprayed on the surface of CNTs films, Janus CNTs-Ecoflex hybrid film was thus obtained after the curing of Ecoflex at room temperature. The CNTs-Ecoflex hybrid film was immersed into the ethanol solution with photoresponsive initiator benzophenone to allow the diffusion of benzophenone into the film, finally the polymerization of NIPAm was initiated on the Ecoflex side in the presence of *N*,*N*′-methylene bisacrylamide (Bis) as the crosslinker to achieve CNTs-Ecoflex/PNIPAm hydrogel composite. The morphology of the hydrogel composite was explored by scanning electronic microscopy (SEM). As shown in Fig. 1b, a porous PNIPAm layer was firmly bonded to a dense Ecoflex layer. To evaluate the combination force between the PNIPAm layer and the Ecoflex layer, 90°-peeling test was carried out. During the peeling test, the top surface of CNTs-Ecoflex (0.1 mm) was stuck on a thin stiff backing, in case of the Ecoflex's elongation along the peeling direction. At the same time, to avoid the sliding of the hydrogel, the bottom surface of the PNIPAm hydrogel (3 mm) was fixed on a thick rigid plate by glue (Fig. S2). As shown in Fig. 1c, the hydrogel composite has a peeling force per unit width of 24 N m^{-1}, moreover, the PNIPAm hydrogel layer was damaged at the interface during the peeling process. The two layers of the hydrogel composite will not separate after repeated ordinary stretching, twisted stretching (Fig. 1e), and it could achieve a maximum tensile stress of 12 kPa with the elongation of about 350% (Fig. 1d). The above results indicate there is strong combination between two layers.

3.2. Thermo-responsive actuation behavior

When the temperature rises above the lower critical solution temperature (LCST) of PNIPAm, the PNIPAm hydrogel layer will undergo a phase change and it will shrink, while the volume of CNTs-Ecoflex will remain unchanged. Because of the strong adhesion between the PNIPAm hydrogel layer and the CNTs-Ecoflex layer, the CNTs-Ecoflex/PNIPAm composite will bend toward the PNIPAm side due to the difference in volume change of both sides. On the contrary, when the temperature is below the LCST of PNIPAm network, PNIPAm hydrogel could swell underwater, and the bilayer hydrogel composite will recover as a result, even bend toward the CNTs-Ecoflex layer. The bending angles were calculated, and bending towards the PNIPAm layer was defined as a positive angle, while bending towards the CNTs-Ecoflex layer was set as a negative angle (Fig. 2a, 2c). The length-width ratio of samples would affect the thermo-triggered bending behaviors (Fig. S3), and the size 15 mm × 3 mm was chosen to realize a circle state in warm water. The influence of the thickness of the PNIPAm hydrogel and the CNTs-Ecoflex film on the actuating performance of the bilayer hydrogel composite was investigated. As shown in Fig. 2b, with the thickness of the CNTs-Ecoflex layer is set as 0.1 mm, when immersed into warm water (40 °C), the bending angle and bending speed of the bilayer hydrogel composite actuator decreasing with increasing thickness of the PNIPAm layer, and when the thickness of the PNIPAm layer is 0.2 mm, the bilayer hydrogel composite only needs 5 s to finish the shape deformation performance. The bending speed is too fast for us to record the process of deformation that we swelled it to a negative angle at first for general operation. It could be speculated that more time is needed for the water molecules to diffuse out of a thick hydrogel layer, which will slow down the actuating speed. When the bilayer hydrogel was transfer to cold water of 20 °C, the PNIPAm layer will swell, and the bilayer hydrogel composite will first recover to a straight state and then gradually bend toward the CNTs-Ecoflex side to achieve a negative bending angle (Figs. S4 and S5). When the thickness the PNIPAm hydrogel layer is set as 0.5 mm, the actuating speeds in both warm water (40 °C) and cold water (40 °C) decrease with the increasing thickness of the CNTs-Ecoflex layer (Figs. 2d and S6, S7). The results indicate that if the CNTs-Ecoflex layer is too thick, it will not be easily driven by the PNIPAm hydrogel layer.

Considering that the strength of CNTs-Ecoflex/PNIPAm composite increases with increasing thickness of hydrogel, we chose CNTs-Ecoflex$_{0.1}$/PNIPAm$_{0.5}$ (the thickness of the Ecoflex layer and the PNIPAm hydrogel layer are 0.1 mm and 0.5 mm, respectively) to perform actuating experiment. As shown in Fig. 2e, an intelligent gripper was fabricated, and it could deform in warm water (40 °C) rapidly and catch a moving object (Movie S1).

3.3. Photothermal actuation behavior

Since CNTs possess near-infrared (NIR) photothermal effect, the temperature of the CNTs-Ecoflex/PNIPAm film would increase with the irradiation of NIR light. As shown in Fig. 3a, the temperature of the bilayer hydrogel composite could reach about 50 °C after exposed to NIR light (808 nm, 1 W/cm^2) for 150 s, which is higher than the LCST of the PNIPAm hydrogel, therefore shape deformation would be realized in air on the basis of the photothermal effect. Taking advantage of the thermo-responsive actuating capacity, an artificial iris was fabricated. As shown in Fig. 3b, with the iris gradually opening in response to the irradiation of NIR light, a flower picture emerges, and the iris could close after turning off the NIR light. Moreover, this actuating behavior shows good repeatability (Fig. S8).

The CNTs-Ecoflex/PNIPAm hybrid film not only possesses photo-responsive actuating performance, but also has electrical conductivity because of the presence of CNTs, and the resistance is about 1.5 MΩ for the 15 mm × 3 mm strip. The bilayer composite was thus applied as an

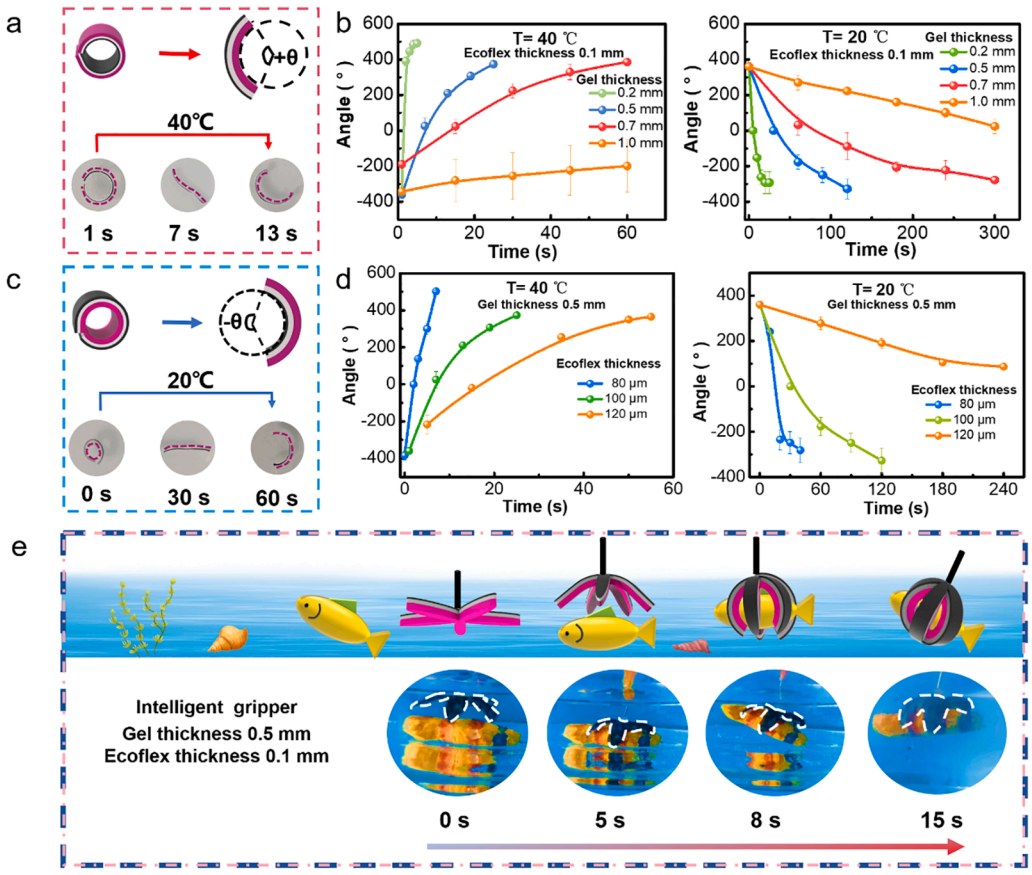

Fig. 2. (a) Schematic illustration and images of the thermo-responsive bending of the CNTs-Ecoflex$_{0.1}$/PNIPAm$_{0.5}$ hydrogel composite (15 mm × 3 mm, 40 °C water bath). (b) The effect of the hydrogel thickness on bending and recovery of the CNTs-Ecoflex$_{0.1}$/PNIPAm$_{y}$ hydrogelcomposite actuators in 40 °C and 20 °C water baths (15 mm × 3 mm). (c) Schematic illustration and images of the thermo-responsive shape recovery of the CNTs-Ecoflex$_{0.1}$/PNIPAm$_{0.5}$ hydrogel composite (15 mm × 3 mm, 20 °C water bath). (d) The effect of the Ecoflex thickness on bending and recovery of the CNTs-Ecoflex$_{x}$/PNIPAm$_{0.5}$ composite actuators in 40 °C and 20 °C water baths (15 mm × 3 mm). (e) Application demonstrations of the CNTs-Ecoflex/hydrogel as an intelligent gripper that could catch a moving fish model in 40 ℃ water bath.

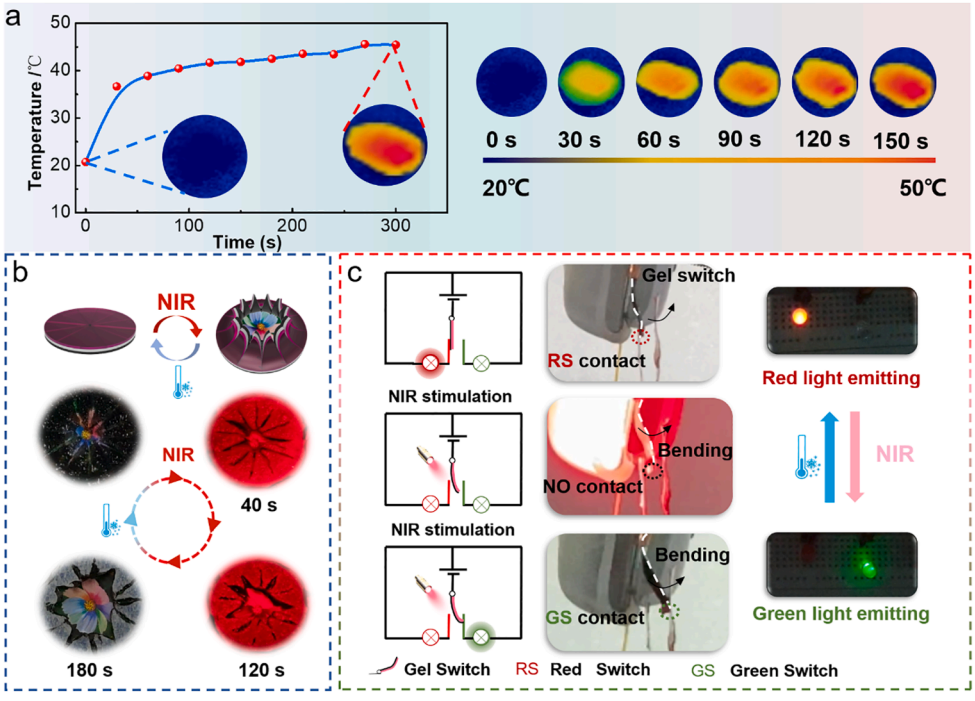

Fig. 3. (a) The temperature increasing of CNTs-Ecoflex/PNIPAm hydrogel film when being irradiated by NIR from 0 to 300 s in air. (b) The Schematic illustration and photos of an artificial iris (CNTs-Ecoflex$_{0.1}$/PNIPAm$_{1}$). (c) The Schematic illustration and photos of the CNTs-Ecoflex$_{0.1}$/PNIPAm$_{0.5}$ as an electric switch to turn on/off red and green lights under NIR irradiation.

electrical switch to turn on/off lights under the influence of NIR irradiation. As displayed in Figs. 3c and S9, S10, the CNTs-Ecoflex/PNIPAm hydrogel composite firstly contacts with the red switch, and the red light is turned on. Then NIR light is applied to generate shape deformation of the bilayer hydrogel composite, it would bend and move away from the red switch and the red light is turned off. Finally, it connects with the green switch, and the green light is thus lit (Movie S2).

3.4. Sensing performance

Since the CNTs-Ecoflex/PNIPAm hydrogel composite exhibits good mechanical stability and conductivity, which encourages us to explore their sensing performance. As can be seen from Fig. 4a, a typical plot for the CNTs-Ecoflex/PNIPAm bilayer composite sensor was tested at different loading conditions by the normalized electrical resistance ($\Delta R/R_0$) change:

$$\Delta R/R_0 = (R - R_0)/R_0 \quad (1)$$

Where R refers to the real-time resistance and R_0 means the initial resistance at the relaxed state (the CNTs-Ecoflex/PNIPAm hydrogel strip with lateral dimensions of 15 mm × 3 mm (length × width)). The corresponding gauge factor (GF) is defined as the relative ratio of ($\Delta R/R_0$) to tensile strain (ε), which was calculated according to Eq. (2):

$$\varepsilon = (L - L_0)/L_0 \quad (2)$$

where L and L_0 refer to the film length at the tensile state and the relaxed state, respectively. The GF was calculated to be 1.34 (ε: 0–60) coupled with a liner response of 0.992. The real-time variation of resistance under repetitive stretching (with ε of 10, 20, 30–40%) was investigated (Fig. 4b), when a tensile strain is applied on the bilayer hydrogel composite, the electric resistance increases, and the signal would recover when the tensile strain released. The hydrogel composite shows good repeatability of the sensing behaviors under each strain. The reliability of the hydrogel composite sensor was further investigated, as shown in Fig. 4c, the bilayer hydrogel composite is applied to continuous stretch-release (ε: 0–20%) for 100 cycles, the electrical resistance shows good stability. Moreover, Fig. 4d confirms that hydrogel composite film has the ability for accurate sensing of deformation, it could detect a series of strain (ε: 10%, 20%, 30%, and 40%) with no obvious overshoot. As shown in Fig. S11 and Movie S3, when a piece of bilayer hydrogel composite is connected in a circuit without stretching, the light bulb is turned on, and when the gel is stretched, the light bulb is dimmed. In addition, the bilayer hydrogel composite could also detect small bending motions as well (Fig. 4e), and the resistance increases with increasing bending angles. As a proof of concept, a hydrogel composite strip was fixed onto the middle finger of a mechanical hand, when the mechanical hand was manipulated to hold a plastic ball, the middle finger would bend, and the resistance would increase (Fig. 4f). The bending angles of the hydrogel composite would be different if the diameter of the plastic ball changes, as displays in Fig. 4f, the value $\Delta R/R$ increases when the size of the plastic ball reduced. These results indicate the hydrogel bilayer composite has reproducible and reliable sensing performance, which could be accurately detected the actuating process in real time.

3.5. The self-sensing and feedback behaviors

The excellent shape deformation and sensing behaviors of the hydrogel bilayer composite encourage us to integrate the actuating and sensing performances. As showed in Fig. 5a and Movie S4, inspired by the contraction and relaxation of biceps, an artificial arm was fabricated by sticking the hydrogel composite strip on two PDMS tubes. When irradiated by NIR light (energy density 1 W/cm^2), in the initial state, the resistance decreases at first because of the photoelectric effect, which is consist with phenomenon we observed in Fig. S12, then the shrinkage of

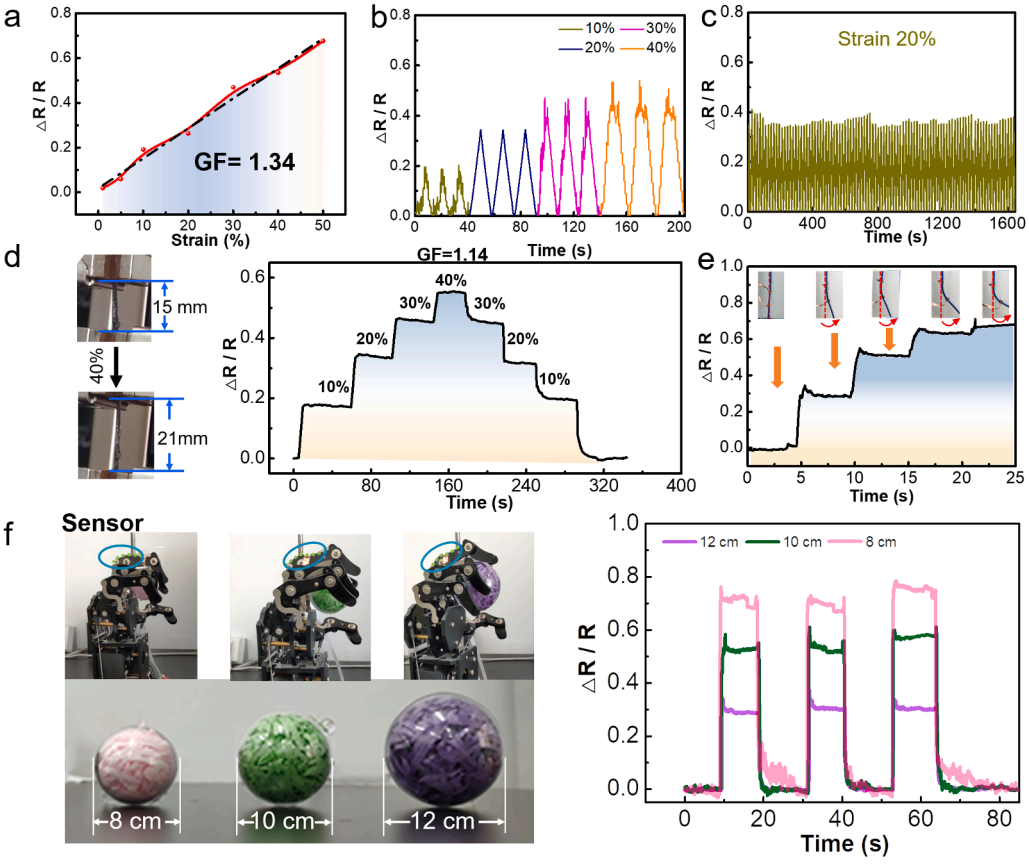

Fig. 4. (a) The sensing performance of the CNTs-Ecoflex$_{0.1}$/PNIPAm$_{0.5}$ hydrogel film with gauge factor. (b) Relative resistance changes ($\Delta R/R_0$) under various cyclical strains (with maximum strains of 10, 20, 30, and 40%, respectively). (c) Cyclic stability test of CNTs-Ecoflex$_{0.1}$/PNIPAm$_{0.5}$ hydrogel film under 20% strain for 100 cycles. (d) Photos and relative resistance changes of CNTs-Ecoflex$_{0.1}$/PNIPAm$_{0.5}$ hydrogel film to stepwise stretching cycles. (e) Photos and Relative resistance changes of CNTs-Ecoflex$_{0.1}$/PNIPAm$_{0.5}$ hydrogel film in response to ruler bending. (f) Resistance response of the middle finger during squeezing balls with different sizes.

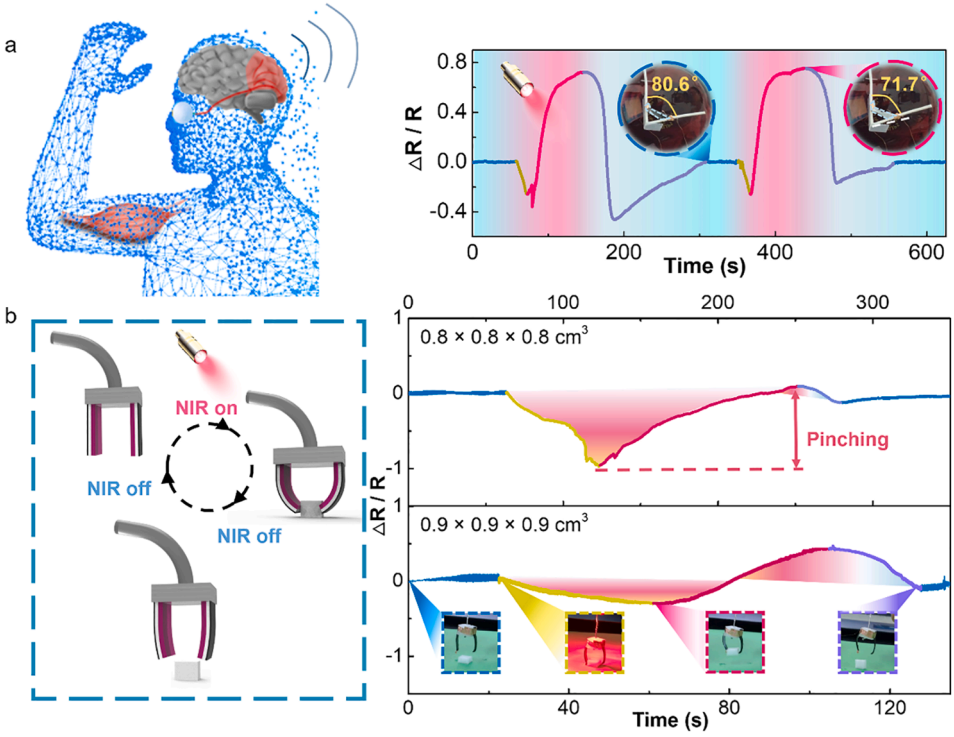

Fig. 5. (a) Photos and resistance responses of an artificial arm. (b) Schematic illustrations and $\Delta R/R_0$-T curves of CNTs-Ecoflex$_{0.1}$/PNIPAm$_{0.5}$ gripper during pinching sponges with different sizes.

the PNIPAm hydrogel would cause the bending of the bilayer hydrogel composite, therefore, the angle between the two PDMS tubes decreases from 80.6° to 71.7° with the resistance gradually increases since the piezoresistive effect. When the resistance closes to stable, it indicates that the motion tends to be maximum, then turned off the NIR, the PNIPAm hydrogel would absorb water from the humid air and swell, therefore, the bilayer hydrogel composite would return to the straight state, and the resistance would decrease to the initial value at the same time. This feedback assists us to detect the maximum actuation state and original straight state. Using the same mechanism, an artificial butterfly that could flap its wings under the irradiation of NIR and be monitored in real time (Fig. S13, Movie S5). Fig. 5b depicts the motions and resistance responses of the bilayer hydrogel composite when it was used as a gripper to catch sponges with different sizes (Movie S6). When the gripper was used to catch smaller object (0.8 × 0.8 × 0.8 cm^3), the change of $\Delta R/R_0$ is lager since it needs to bend more than to catch a larger object (0.9 × 0.9 × 0.9 cm^3). These results confirm that actuating and real-time sensory feedback could be integrated perfectly.

4. Conclusions

In summary, we have developed a novel bilayer hydrogel composite actuator with integrated sensing performance. The hydrogel composite was fabricated by growing PNIPAm hydrogel layer on a Janus CNTs-Ecoflex hybrid film, the thermo-responsiveness of the PNIPAm hydrogel layer renders the hydrogel composite shape deformation capacity upon the trigger of heat, while the CNTs layer endow the hydrogel composite with sensing ability. Moreover, taking advantage of the photothermal conversion performance of CNTs, integrated actuating and sensing behaviors could be achieved with the assistance of NIR. We believe our strategy will inspire the design and fabrication of novel intelligent systems with actuating and feedback sensing behaviors.

Declaration of Competing Interest

The authors declare that they have no known competing financial interests or personal relationships that could have appeared to influence the work reported in this paper.

Acknowledgements

This work was supported by National Natural Science Foundation of China (51873223, 52073295), Youth Innovation Promotion Association of Chinese Academy of Sciences (2017337), Open Research Fund of Key Laboratory of Marine Materials and Related Technologies (2020K05), Ningbo Natural Science Foundation (202003N4359), Ningbo Scientific and Technological Innovation 2025 Major Project (2018B10057).

Appendix A. Supplementary data

Supplementary data to this article can be found online at https://doi.org/10.1016/j.cej.2021.128988.

References

[1] C.J. Yu, Z. Duan, P.X. Yuan, Y.H. Li, Y.W. Su, X. Zhang, Y.P. Pan, Lenore L. Dai, Ralph G. Nuzzo, Y.G. Huang, H.Q. Jiang, John A. Rogers, Electronically programmable, reversible shape change in two- and three-dimensional hydrogel structures, Adv. Mater. 25 (2013) 1541–1546, https://doi.org/10.1002/adma.201204180.
[2] L. Zong, X.K. Li, X.S. Han, L.L. Lv, M.J. Li, J. You, X.C. Wu, C.X. Li, Activation of actuating hydrogels with WS_2 nanosheets for biomimetic cellular structures and steerable prompt deformation, ACS Appl. Mater. Interfaces 9 (2017) 32280–32289, https://doi.org/10.1021/acsami.7b10348.
[3] C. Ma, X. Le, X. Tang, J. He, P. Xiao, J. Zheng, H.e. Xiao, W. Lu, J. Zhang, Y. Huang, T. Chen, A multiresponsive anisotropic hydrogel with macroscopic 3D complex deformations, Adv. Funct. Mater. 26 (2016) 8670–8676, https://doi.org/10.1002/adfm.201603448.
[4] X. Li, X.B. Cai, Y.F. Gao, M.J. Serpe, Reversible bidirectional bending of hydrogel-based bilayer actuators, J. Mater. Chem. B 5 (2017) 2804–2812, https://doi.org/10.1039/C7TB00426E.

[5] Y.C. Zhang, J.X. Liao, T. Wang, W.X. Sun, Z. Tong, Polyampholyte hydrogels with pH modulated shape memory and spontaneous actuation, Adv. Funct. Mater. 28 (2018) 1707245, https://doi.org/10.1002/adfm.201707245.
[6] Z.L. Han, P. Wang, G.Y. Mao, T.H. Yin, D.M. Zhong, B. Yiming, X.C. Hu, Z. Jia, G. D. Nian, S.X. Qu, W. Yang, Dual pH-responsive hydrogel actuator for lipophilic drug delivery, ACS Appl. Mater. Interfaces 12 (2020) 12010–12017, https://doi.org/10.1021/acsami.9b21713.s003.
[7] K. Iwaso, Y. Takashima, A. Harada, Fast response dry-type artificial molecular muscles with [c2]daisy chains, Nat. Chem. 8 (2016) 625–632, https://doi.org/10.1038/nchem.2513.
[8] Y.S. Zhao, C. Xuan, X.S. Qian, Y. Alsaid, M.T. Hua, L.H. Jin, X.M. He, Soft phototactic swimmer based on self-sustained hydrogel oscillator, Sci. Robot. 4 (2019) eaax7112, https://doi.org/10.1126/scirobotics.aax7112.
[9] C.X. Ma, W. Lu, X.X. Yang, J. He, X.X. Le, L. Wang, J.W. Zhang, M.J. Serpe, Y. J. Huang, T. Chen, Bioinspired anisotropic hydrogel actuators with on-off switchable and color-tunable fluorescence behaviors, Adv. Funct. Mater. 28 (2018) 1704568, https://doi.org/10.1002/adfm.201704568.
[10] L. Zhao, J.H. Huang, Y.C. Zhang, T. Wang, W.X. Sun, Z. Tong, Programmable and bidirectional bending of soft actuators based on janus structure with sticky tough PAA-clay hydrogel, ACS Appl. Mater. Interfaces 9 (2017) 11866–11873, https://doi.org/10.1021/acsami.7b00138.s005.
[11] D. Han, C. Farino, C. Yang, T. Scott, D. Browe, W. Choi, J.W. Freeman, H. Lee, Soft robotic manipulation and locomotion with a 3D printed electroactive hydrogel, ACS Appl. Mater. Interfaces 10 (2018) 17512–17518, https://doi.org/10.1021/acsami.8b04250.s005.
[12] B. Xue, M. Qin, T.K. Wang, J.H. Wu, D.J. Luo, Q. Jiang, Y. Li, Y. Cao, W. Wang, Electrically controllable actuators based on supramolecular peptide hydrogels, Adv. Funct. Mater. 26 (2016) 9053–9062, https://doi.org/10.1002/adfm.201603947.
[13] S.W. Xiao, M.Z. Zhang, X.M. He, L. Huang, Y.X. Zhang, B.P. Ren, M.Q. Zhong, Y. Chang, J.T. Yang, J. Zheng, Dual salt- and thermoresponsive programmable bilayer hydrogel actuators with pseudo-interpenetrating double-network structures, ACS Appl. Mater. Interfaces 10 (2018) 21642–21653, https://doi.org/10.1021/acsami.8b06169.s003.
[14] Z.F. Sun, Y. Yamauchi, F. Araoka, Y.S. Kim, J. Bergueiro, Y. Ishida, Y. Ebina, T. Sasaki, T. Hikima, T. Aida, An anisotropic hydrogel actuator enabling earthworm-like directed peristaltic crawling, Angew. Chem. Int. Ed. 57 (2018) 15772–15776, https://doi.org/10.1002/anie.201810052.
[15] X.S. Qian, Y.S. Zhao, Y. Alsaid, X. Wang, M.T. Hua, T. Galy, H. Gopalakrishna, Y. Y. Yang, J.S. Cui, N. Liu, M. Marszewski, L. Pilon, H.Q. Jiang, X.M. He, Artificial phototropism for omnidirectional tracking and harvesting of light, Nat. Nanotechnol. 14 (2019) 1048–1055, https://doi.org/10.1038/s41565-019-0562-3.
[16] H. Yuk, S.T. Lin, C. Ma, M. Takaffoli, N.X. Fang, X.H. Zhao, Hydraulic hydrogel actuators and robots optically and sonically camouflaged in water, Nat. Commun. 8 (2017), https://doi.org/10.1038/ncomms14230.
[17] A.S. Gladman, E.A. Matsumoto, R.G. Nuzzo, L. Mahadevan, J.A. Lewis, Biomimetic 4D printing, Nat. Mater. 15 (2016) 413–418, https://doi.org/10.1038/nmat4544.
[18] J.R. Wang, J.F. Wang, Z. Chen, S.L. Fang, Y. Zhu, R.H. Baughman, L. Jiang, Tunable, fast, robust hydrogel actuators based on evaporation-programmed heterogeneous structures, Chem. Mater. 29 (2017) 9793–9801, https://doi.org/10.1021/acs.chemmater.7b03953.s003.
[19] Z. Li, P.C. Liu, X.F. Ji, J.Y. Gong, Y.B. Hu, W.J. Wu, X.N. Wang, H.Q. Peng, R.T. K. Kwok, J.W.Y. Lam, J. Lu, B.Z. Tang, Bioinspired simultaneous changes in fluorescence color, brightness, and shape of hydrogels enabled by AIEgens, Adv. Mater. 32 (2020) 1906493, https://doi.org/10.1002/adma.201906493.
[20] S.X. Wei, W. Lu, X.X. Le, C.X. Ma, H. Lin, B.Y. Wu, J.W. Zhang, P. Theato, T. Chen, Bioinspired synergistic fluorescence-color-switchable polymeric hydrogel actuators, Angew. Chem. Int. Ed. 58 (2019) 16243–16251, https://doi.org/10.1002/anie.201908437.
[21] L. Wang, Y.K. Jian, X.X. Le, W. Lu, C.X. Ma, J.W. Zhang, Y.J. Huang, C. Feng Huang, T. Chen, Actuating and memorizing bilayer hydrogels for a self-deformed shape memory function, Chem. Commun. 54 (2018) 1229–1232, https://doi.org/10.1039/C7CC09456F.
[22] J. Zheng, P. Xiao, X.X. Le, W. Lu, P. Théato, C.X. Ma, B.Y. Du, J.W. Zhang, Y. J. Huang, T. Chen, Mimosa inspired bilayer hydrogel actuator functioning in multi-environments, J. Mater. Chem. C 6 (2018) 1320–1327, https://doi.org/10.1039/C7TC04879C.
[23] Y.H. Bi, X.X. Du, P.P. He, C.Y. Wang, C. Liu, W.W. Guo, Smart bilayer polyacrylamide/DNA hybrid hydrogel film actuators exhibiting programmable responsive and reversible macroscopic shape deformations, Small 16 (2020) 1906998, https://doi.org/10.1002/smll.201906998.
[24] T.T. Chen, H. Bakhshi, L. Liu, J. Ji, S. Agarwal, Combining 3D printing with electrospinning for rapid response and enhanced designability of hydrogel actuators, Adv. Funct. Mater. 28 (2018) 1800514, https://doi.org/10.1002/adfm.201800514.
[25] H.J. Lin, S.H. Ma, B. Yu, X.W. Pei, M.R. Cai, Z.J. Zheng, F. Zhou, W.M. Liu, Simultaneous surface covalent bonding and radical polymerization for constructing robust soft actuators with fast underwater response, Chem. Mater. 31 (2019) 9504–9512, https://doi.org/10.1021/acs.chemmater.9b03670.s009.
[26] X.M. He, Y. Sun, J.H. Wu, Y. Wang, F. Chen, P. Fan, M.Q. Zhong, S.W. Xiao, D. Zhang, J.T. Yang, J. Zheng, Dual-stimulus bilayer hydrogel actuators with rapid, reversible, bidirectional bending behaviors, J. Mater. Chem. C 7 (2019) 4970–4980, https://doi.org/10.1039/C9TC00180H.
[27] Q. Shi, H. Xia, P. Li, Y.S. Wang, L. Wang, S.X. Li, G. Wang, C. Lv, L.G. Niu, H.B. Sun, Photothermal surface plasmon resonance and interband transition-enhanced nanocomposite hydrogel actuators with hand-like dynamic manipulation, Adv. Opt. Mater. 5 (2017) 1700442, https://doi.org/10.1002/adom.201700442.
[28] Y. Zhou, A.W. Hauser, N.P. Bende, M.G. Kuzyk, R.C. Hayward, Waveguiding microactuators based on a photothermally responsive nanocomposite hydrogel, Adv. Funct. Mater. 26 (2016) 5447–5452, https://doi.org/10.1002/adfm.201601569.
[29] M.T. Li, X. Wang, B. Dong, M. Sitti, In-air fast response and high speed jumping and rolling of a light-driven hydrogel actuator, Nat. Commun. 11 (2020), https://doi.org/10.1038/s41467-020-17775-4.
[30] R.C. Luo, J. Wu, N.D. Dinh, C.H. Chen, Gradient porous elastic hydrogels with shape-memory property and anisotropic responses for programmable locomotion, Adv. Funct. Mater. 25 (2015) 7272–7279, https://doi.org/10.1002/adfm.201503434.
[31] P. Xiao, J.C. Gu, C.J. Wan, S. Wang, J. He, J.W. Zhang, Y.J. Huang, S.W. Kuo, T. Chen, Ultrafast formation of free-standing 2D carbon nanotube thin films through capillary force driving compression on an air/water interface, Chem. Mater. 28 (2016) 7125–7133, https://doi.org/10.1021/acs.chemmater.6b03420.s004.